Attitude Detection of Buccaneer RMM CubeSat through Experimental and Simulated Light Curves in combination with Telemetry Data

M. Cegarra Polo, R. Abay, S. Gehly, A. Lambert, P. Lorrain, S. Balage, M. Brown and C. Bright

School of Engineering and IT, UNSW Canberra Space, Canberra, Australia

ABSTRACT

Identification and characterisation of the growing population of resident space objects (RSOs) in orbit around Earth is central to current and future Space Traffic Management and Space Situational Awareness (SSA) activities. Research at University of New South Wales (UNSW) Canberra Space seeks to assist this effort through combining optical measurements of selected RSOs with numerical astrodynamics modelling techniques to extend the information that can be inferred about an RSO from its photometric light curve signature.

The initial phase of this research comprised two three-month observation campaigns, which were completed in July 2018. A collection of photometric light curves was obtained using different nodes of the Falcon Telescope Network (FTN) for the Buccaneer Risk Mitigation Mission (BRMM) 3U CubeSat. The BRMM was launched in 2017 as a joint mission between UNSW Canberra Space and the Defence Science and Technology Group (DST). While BRMM is a pathfinder for the future Buccaneer Main Mission whose primary objective will be the calibration of the Jindalee Operational Radar Network (JORN), it also serves as a stepping stone in building Australian space capability. For BRMM one of the mission objectives was to perform photometric experiments to contribute to SSA research and development efforts via dynamic on-orbit manoeuvres. This paper reports on the initial analysis of the photometric light curves central to the SSA mission goal. The material properties and dynamic attitude motion of the BRMM during the FTN observations are known, with rotational body rates commanded from 0.2 to 5 degrees per second about multiple combinations of body axes to build a comprehensive database of light curves for analysis. Further variation in the light curve database is provided by observations obtained prior to solar panel and antenna deployment.

A set of 70 light curves was obtained during the observational campaigns, with each light curve signature containing a bulk change in intensity over time due to the change in range as BRMM approaches the FTN node on its Low Earth Orbit (LEO) trajectory. Superimposed on the mean intensity change are characteristic peaks and troughs produced by reflections from individual facets of the spacecraft, the magnitude and frequency of which are highly dependent upon the spacecraft's attitude and body rate. Samples from the light curve database are presented with the attitude data downlinked from the spacecraft to assess light curve variations with attitude and spin rate of the spacecraft.

Supporting the optical data are numerically simulated light curves, generated by applying the Ashikhmin-Premože Bidirectional Reflectance Distribution Function (BRDF) Model for the BRMM geometry using a high-fidelity 6 Degree of Freedom (DOF) orbit propagator supported by the Orekit orbit propagation library for computations related to time systems, coordinate frames, and gravitational perturbations. The performance of the numerical simulation was evaluated by superimposing the attitude profile reported by the spacecraft telemetry on top of the propagated orbit to provide a one-to-one comparison between the measured and simulated light curves for select cases.

A preliminary investigation into the feasibility of using the simulation tool to infer attitude dynamics from a given light curve signature is also presented. A candidate set of simulated light curves was generated by numerically propagating a set of initial attitude states and constant body rates through the observation window. The results were searched to find the case that provided the best fit to the observed light curve. A further study was initiated to investigate the errors introduced by the assumption of a constant body rate throughout the observation for the simulated light data.

1 INTRODUCTION

Small satellites show a relatively high mission failure rate during their lifetime compared with other spacecraft, which combined with the fact that most of them don't have effective thrust systems, makes them a potential source of space debris in the currently overcrowded LEO orbit. This issue has been aggravated in recent years by the growth of this type of satellite and this trend seems unlikely to diminish, with approximately 120 from a

total number of 587 small satellites currently in orbit in a non-operational status. Predictions indicate that more than 3000 small satellites will be launched within the next five years [1].

These figures indicate that the probability of unidentified and uncontrolled objects in space is higher, with the subsequent risk of collisions with other spacecrafts, especially in LEO, which is where most CubeSats are found. Though these objects are monitored by the Joint Space Operations Center (JSpOC), any effort towards the fast identification after launch, accurate orbit prediction, attitude, and deployment status of the spacecraft can be very useful.

Mission operators typically use on-board sensors to determine the attitude of the spacecraft and its position in space, or the deployment status of appendages. The sensor telemetry is then acquired via a radio link with the ground. This information is often not available if the spacecraft is in an uncontrolled state and alternative methods are necessary to locate and assess the status of the spacecraft. These methods include Satellite Laser Ranging (SLR) [2] and inverse synthetic aperture radar (ISAR) [3], which coexist with photometric light curve analysis using ground-based telescopes, with heritage from shortly after the first satellite reached orbit in 1957.

Some authors have explored the use of photometric light curves to detect the attitude of CubeSats. Pittet correlated light curve photometric observations of the SwissCube spacecraft with three different data sources to detect its spin rate: radio signals, on-board gyroscopes, and on-board sun sensors. Results of this research show a correlation in the spin rate measurements when the spin period was under 60 seconds [4]. Gasdia was able to produce photometric information from CubeSats up to about 10 Hz time resolution, with an inexpensive and portable platform based in commercial-off-the-shelf (COTS) hardware [5]. They showed a set of controlled and uncontrolled small satellite light curves that exhibited glints with different periodicity, where they established relationships between these periodic flashes and their nominal spin rates.

This paper evaluates the feasibility of using light curves in combination with astrodynamics and BRDF models in addition to telemetry data, as a reliable way to detect the spin rates, attitude, and deployment status of solar panels and antennas of a small satellite in LEO orbit. For that purpose, we have performed photometric analysis of the BRMM CubeSat, which was launched in November 2017. We analyse attitude and spin rates of the BRMM using three different data sources: experimental light curves based on telescope observations, telemetry downloaded during the BRMM passes, and simulated light curves based on an Ashikhmin-Premože BRDF model [6]. Comparing experimental light curves with telemetry and simulations can be useful to validate the attitude and spin rate of the spacecraft at times when telemetry is not available. This work could be generalised for many of the CubeSats in LEO, with almost half of those currently in orbit sharing the 3U form factor of the BRMM CubeSat [1].

Section 2 of this document describes the main features of BRMM CubeSat and its orbital parameters. In section 3 a short description of the FTN network of telescopes from USAFA is shown. Section 4 describes the observation campaigns, the different experiments carried out, and the parameters and telescope configuration used for the photometric observations. Finally, section 5 includes the results achieved in the different analysis and experiments performed.

2 BUCCANEER RISK MITIGATION MISSION CUBESAT

The BRMM 3U CubeSat, shown in Fig. 1, serves as a pathfinder for the Buccaneer Main Mission and has been designed, built, tested, and jointly operated by UNSW Canberra Space and DST [7, 8]. The key mission objectives are to

1. Undertake and monitor the complex commissioning of a high frequency receiver and antenna to be used in the Main Mission for the Jindalee Operational Radar Network (JORN) calibration.
2. Perform photometric experiments to contribute to SSA research and development efforts via dynamic manoeuvres on-orbit.
3. Further develop Australian expertise in small-satellite development and operations.

The BRMM (NORAD 43014, international designator 2017-073B) was launched on 18th November 2017 at approximately 11:47 UTC from Vandenberg Air Force Base in California as part of the ELaNa-XIV launch. Table 1 shows the nominal orbital parameters.

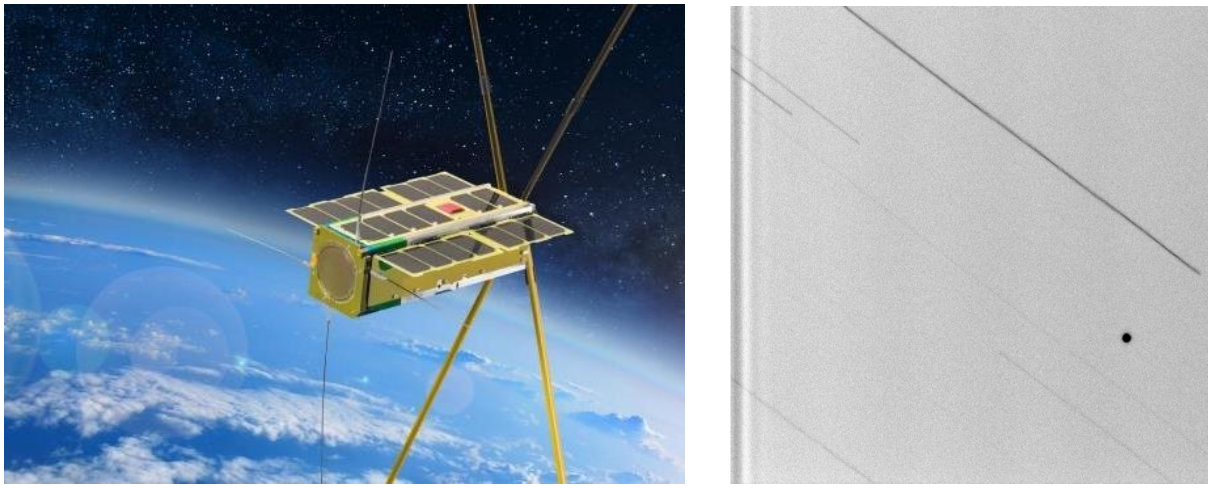

Fig. 1. (Left) The BRMM CubeSat (artist impression. Source: https://newsroom.unsw.edu.au). (Right) Image (negative) of the BRMM CubeSat taken with FTN NJC Telescope the 27th of June 2018 at 07:58:30 UTC.

Table 1. The BRMM CubeSat nominal orbital parameters.

Apogee	811 km
Perigee	440 km
Inclination	97.73°
LTAN (Local Time of Ascending Node)	13:20:35 hours

One of the critical elements of the spacecraft is the large High Frequency (HF) antenna, which consists of four elements of carpenter's measuring tape, each 1.7 m long. The antenna elements are arranged in an X-shaped configuration, which was stowed prior to launch and successfully deployed in several stages between 16th and 26th of April 2018. The spacecraft body coordinate system is illustrated in Fig. 2.

The on-board Attitude Determination and Control System (ADCS) is a MAI-400 unit, which provides three-axis pointing using three-axis reaction wheels, electromagnets, a magnetometer, six course sun sensors, 3-axis MEMS accelerometer gyroscope, Earth horizon sensors, and an ADACS computer.

The BRMM is jointly operated from ground stations in Australia: DST Edinburgh and UNSW Canberra. Telemetry for these experiments was downlinked to the ground stations, with attitude and body rate data available at a sample frequency of up to 1 Hz.

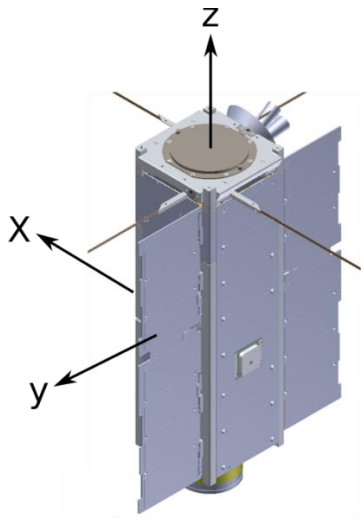

Fig. 2. Illustration of the BRMM body coordinate system.

3 FALCON TELESCOPE NETWORK

The FTN is a global array of twelve telescopes spread around four continents developed by the Center for Space Situational Awareness Research in the Department of Physics at United States Air Force Academy (USAFA) [9]. Strategic location of the nodes enables continuous or simultaneous observations of a single object in the sky. Telescopes can be used on-site or remotely, but the primary use is through scheduled observations that the FTN partners submit in a web-based interface, from which images can be downloaded after the observation sessions. Fig. 3 shows the location of the FTN observatories used in this research.

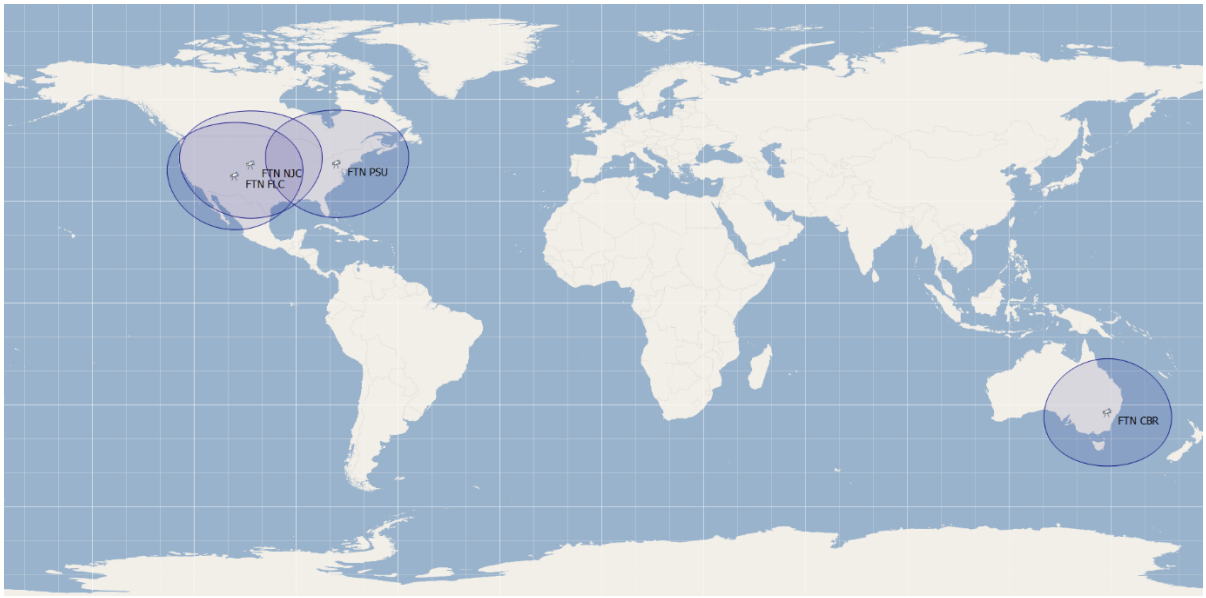

Fig. 3. Location of the four FTN telescopes (FTN CBR, FTN FLC, FTN PSU, FTN NJC) used in this research (coverage in blue).

Each observatory is equipped with a ProRC 500 Officina Stellare telescope (0.5 m diameter of primary mirror and focal ratio F/8) installed in a Paramount ME II Robotic Mount, an Apogee Alta F47 CCD camera mounted in prime focus, a set of seven Johnson-Cousin and Sloan prime filters plus an additional ExoPlanet Blue-Blocking filter, and a Richardson transmission diffraction grating (100 lines/mm). A ViewFinder Scope is mounted in a piggyback configuration on top of the main scope, with an ATIK 414ex monochrome camera in its prime focus. TPoint is the software used to correct pointing and tracking, where a pointing accuracy of 15 arcsec RMS in some of the nodes has been achieved.

4 DESCRIPTION OF OBSERVATIONAL CAMPAIGNS, EXPERIMENTS AND TELESCOPE CONFIGURATIONS

Due to the orbital parameters of the spacecraft and the Earth's tilt relative to the sun, BRMM is visible from different FTN nodes at different times of the year. We studied BRMM during two observational campaigns: first from November 2017 to February 2018 from FTN Canberra, and second from May 2018 to July 2018 from US FTNs in Colorado and Pennsylvania. From FTN Canberra its Sun-lit segment starts at a certain altitude until it disappears below the horizon in the South, whereas from US FTNs telescopes, its sun-lit segment starts at the horizon and enters the Earth shadow at a certain altitude. The pass on the 5th of January 2018 BRMM could be observed from FTN Canberra at its maximum elevation, 54°, at a slant range of 946 km. The pass on the 11th of June 2018 BRMM could be observed from US FTNs at its maximum elevation, 89°, at a slant range of 802 km. Passes observed from FTN Canberra had a maximum duration of approximately 4 minutes, whereas from US FTNs maximum duration was approximately 7 minutes.

FTN telescopes include the same equipment in all nodes, so there is no need to calibrate photometric results obtained with different telescopes, provided that the same parameters are used for all observations. Nevertheless, the seeing of each site can be different, due to light pollution, atmospheric turbulence profile, site altitude, and weather conditions on the night. The ExoPlanet filter was selected for BRMM observations because from all filters installed in FTN nodes, it is the one that allows most of the light to come through, and the interest of this project was not the spectral content of the signal, but the improvement of the light curve time resolution by reducing the exposure time. This allowed the use of an exposure time of one second in most of the

passes during the second campaign, when the solar panels and HF antenna were deployed, which produced a reasonable Signal to Noise Ratio (SNR) in the image sensor. On the contrary, light curves obtained from FTN Canberra had a minimum exposure time of five seconds, due to the lower cross-sectional area of the spacecraft observed from the telescope site when the HF antenna and solar panels were not deployed. Considering that the readout time of the image sensor needs to be added to its exposure time, the maximum frame rate in the best case is 0.3 Hz. With such a frame rate, the light curve won't detect fast changes in spacecraft rotation rate, but telemetry shows rotation rates up to 5 degrees per second, which is slow enough to generate detectable periodic glints in the experimental light curves.

When possible, BRMM was observed simultaneously with the main scope and the ViewFinder of each FTN node. Observations with the ViewFinder were useful to better locate the spacecraft due to its wider Field of View (FOV) of 30 arcmins, compared with the 11 arcmins FOV of the main scope.

In most of the passes, the spacecraft was not driven by commands from the ground stations, so body rates were assumed to be constant during the pass, therefore detected periodic glints in the light curve should have a relationship with the combination of the three body rates of each of the rotation axes of BRMM. Apart from the constant body rate passes, there were a series of deliberate spin-up experiments, which consisted of the following configurations during several different passes:

- Y reaction wheel spinning at 7500 rpm.
- Y reaction wheel spinning at 2500 rpm
- Y reaction wheel spinning at 9000 rpm and then changed to 0 rpm during the pass.
- Y and Z reaction wheels spinning at 9000 rpm.

5 RESULTS

5.1 Detection of solar panels and HF antenna deployment

The two observational campaigns were carried out before and after April 2018, when solar panels and HF antenna were deployed. The reflective areas that contribute to the photometric flux received in the telescope image sensor are different in the two campaigns due to the different antenna and solar panels deployment status.

The form factor of BRMM is 3U, including two stackable solar panels in YZ plane and a X-shaped HF antenna in XY plane (see fig. 2). The increase in the light collecting area in the spacecraft after deployment should correspond to an increase in the photometric measurements in the telescope.
The maximum area in the spacecraft before deployment is a 3U segment, whereas after deployment the maximum area is a 9U segment, which is 3 times bigger. The HF antenna, though large enough (4 segments of 1.7 metres), has curved surfaces so we expect that its contribution is less than the flat surfaces of the spacecraft facets.

To compare photometric measurements before and after deployment, we first normalize the received flux to 5 seconds exposure time, considering that the CCD camera shows a linear behaviour. We then remove the influence of the slant range, taking into account that the apparent brightness of a light source is inversely proportional to the square of its distance, normalising the received flux in the telescope for an object situated at a slant range of 1000 km. After this adjustment, we represent in figure 4 the relation between the solar phase angle and peak values of the photometric measurements before and after deployment, where each dot of the scatter plot represents one observation.

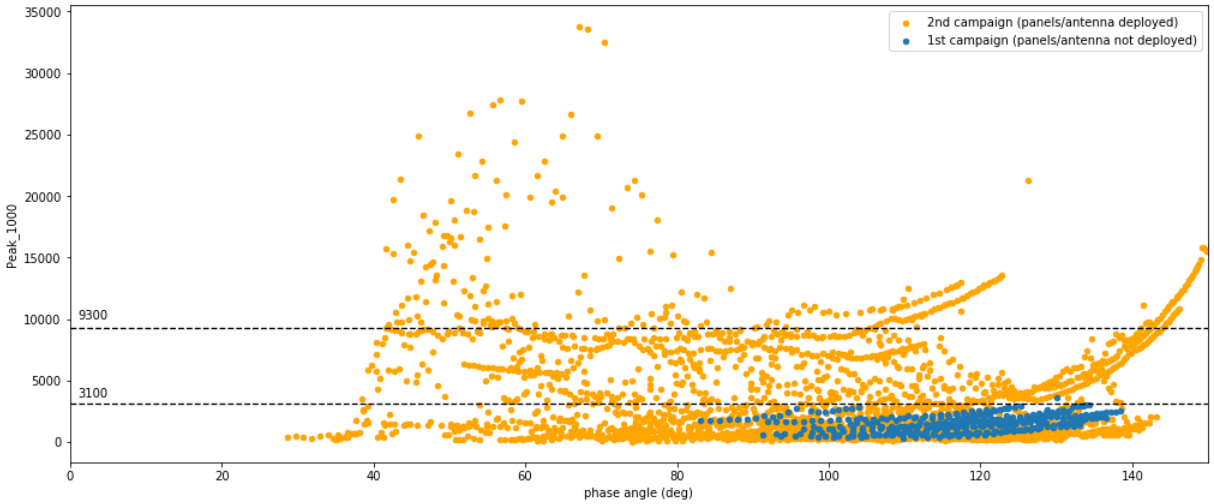

Fig. 4. Peaks (units in pixels counts) of each photometric observation as a function of solar phase angle.

It can be appreciated that the relation between the maximum values for the same phase angle range of both sets is in a factor of around 3, which is the expected photometric relation with the maximum reflective areas of the spacecraft. Nevertheless, in this study the atmospheric extinction hasn't been considered and neither the different turbulence profiles of the different telescope sites, which will require further study.

We can detect deployment of structures in the spacecraft with certain degree of uncertainty, provided we have enough photometric measurements, and assuming that the spacecraft is rotating around its three axes, which will cover all possible relative attitudes respect to the observer.

5.2 Comparison of simulated and experimental light curves

Six passes were observed by FTN NJC (sited in Sterling, US) in June. Telemetry data including attitude states for all the passes were available. Two different analyses were conducted using the simulated and experimental light curves. In the first analysis the simulated light curves from the telemetry attitude orientation data are compared to the experimental light curves for the validation of 6DoF propagator and BRDF model. Although six visible passes were rigorously investigated, a high rotation rate (06 June) and a low rotation rate (05 June) cases are presented in this paper.

The second analysis shows the comparison of the power spectra of both experimental and simulated light curves with the telemetry body rates. To obtain the power spectra we use the Lomb-Scargle (LS) periodogram. This is a commonly used method to detect periodic signals in unevenly-spaced observations, which is the case of this research. This is due to the different exposure times and varying readout times in the CCD camera, that prevent the use of more common analysis tools, such as the fast Fourier transform, that needs equally spaced signals in the time domain. The implementation used here is a python package included in Astropy python library [10].

5.2.1 Simulated flux from quaternion estimated in the telemetry vs. experimental light curves

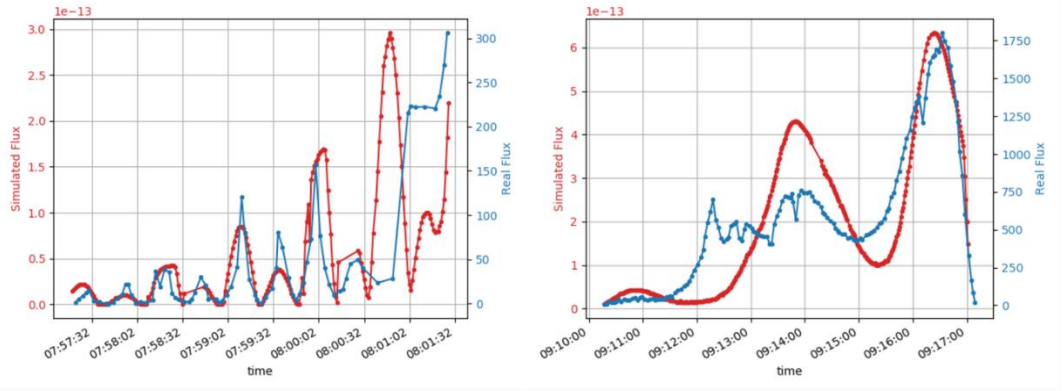

Fig. 6. June 06 pass (Left) and June 05 pass (Right) simulated versus experimental light curves. Simulated flux in watts/m^2.

Simulated flux from attitude states in the telemetry data were plotted against experimental light curves to validate the developed 6DoF propagator [11]. Fig.6 shows that there is an evident match between simulated and experimental light curves, and this is quite good result given the material properties of the Buccaneer are assumed to be uniform for all facets. It should be noted that both the simulated and experimental light curves are shown without any processing. The phase shift between experimental and simulated light curves can be due to the integration time of the telescope, minor time differences between spacecraft and ground station clocks, TLE uncertainties or other causes that need to be explored in future research.

5.2.2 Experimental and simulated light curves power spectra vs. rotational body rates from telemetry

In order to relate the glints periodicity observed in the experimental light curves with the rotational status of the spacecraft, we compare the main frequencies of these light curves obtained with the Lomb-Scargle periodogram with the body rates extracted from the telemetry.

We also perform a similar process with the simulated light curves obtained from the estimated quaternion from the telemetry, to measure how well the developed 6DoF propagator simulates the spectral content of the signal.

For that purpose, we performed this analysis for two different passes with different readings in the telemetry body rates, which results are shown in fig. 7 and 8.

Table 3 shows the body rates results from the three different analysis: experimental light curves, simulated light curves and telemetry.

Table 3. Body rates from different analyses in deg/s.

Pass	LS Experimental	LS Simulated	Telemetry (mean)
6 June	3.24	2.28	3.66
5 June	0.67	0.64	0.84

In general terms, body rates extracted from the three different analyses show relative similarity on their values, and differences can be portrayed to different noise sources: photometric calibration of images, LS periodogram accuracy or telemetry sensor noise on the spacecraft.

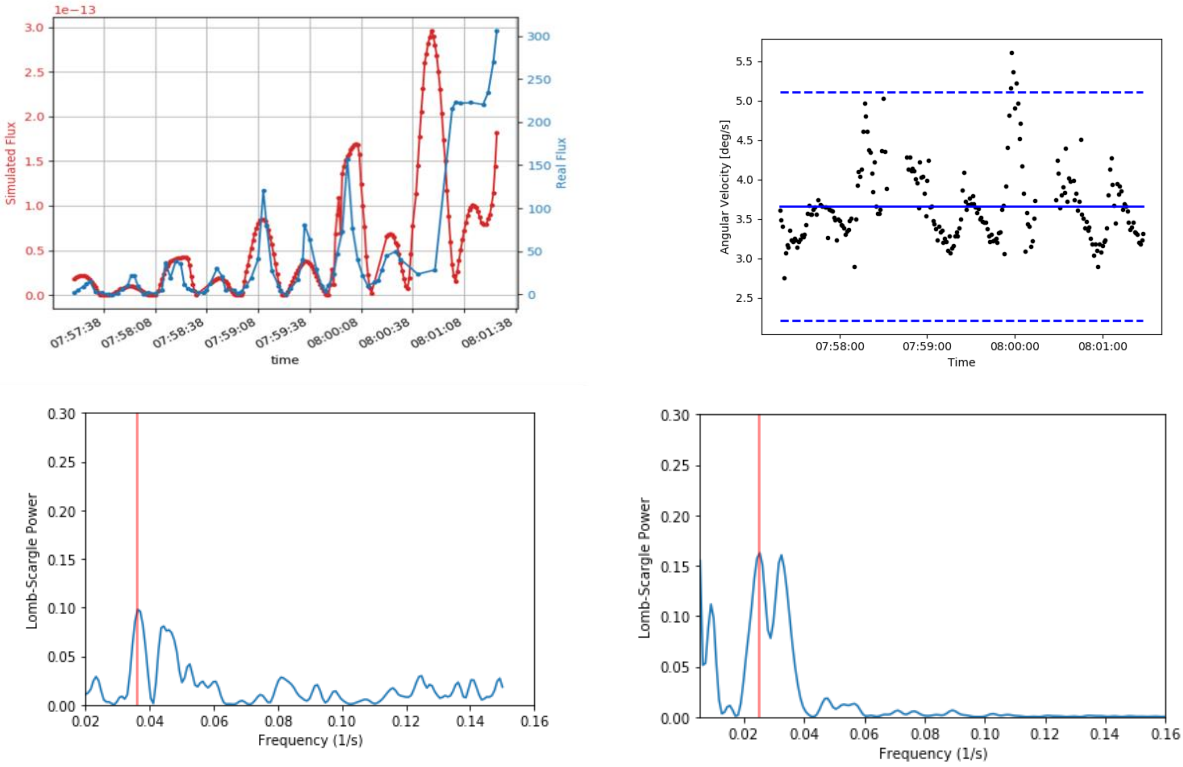

Fig. 7. Pass 1 of 06-June-2018. Experimental (blue) and simulated (red) light curves (top left). RSS body rates from telemetry (top right). Lomb-Scargle periodogram of experimental light curve (bottom left). Lomb-Scargle periodogram of simulated light curve (bottom right). Simulated flux in watts/m^2.

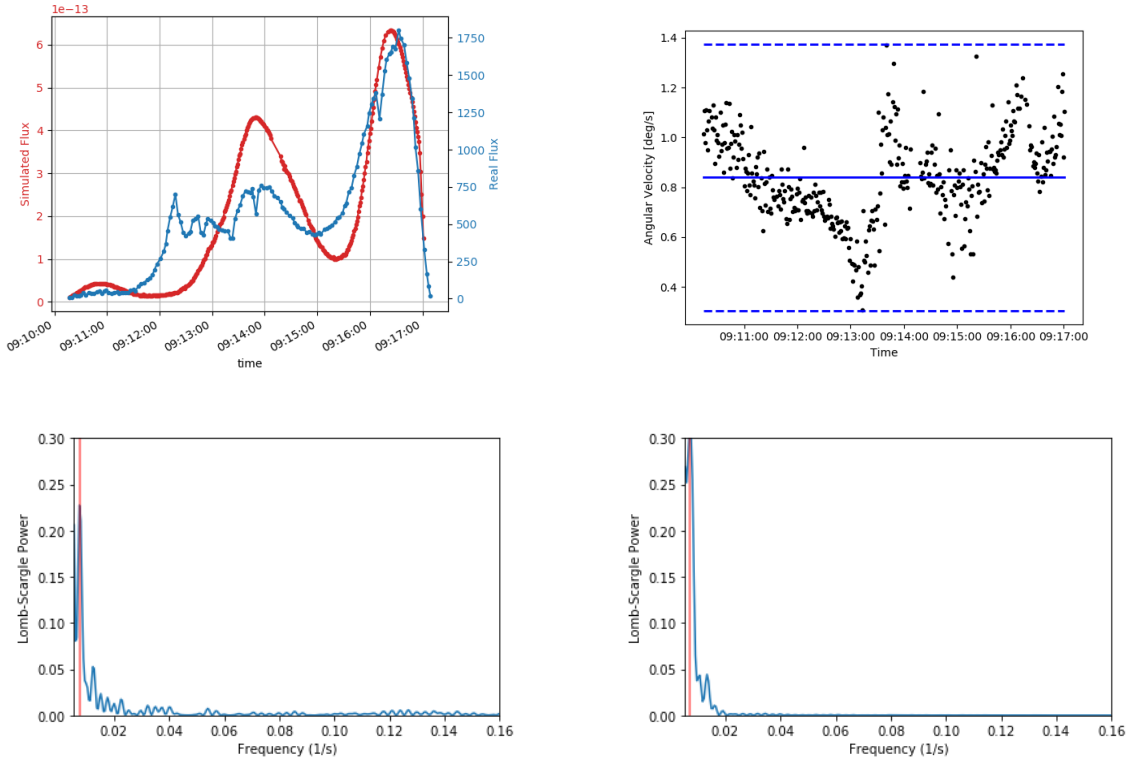

Fig. 8. Pass 2 of 05-June-2018. Experimental (blue) and simulated (red) light curves (top left). RSS body rates from telemetry (top right). Lomb-Scargle periodogram of experimental light curve (bottom left). Lomb-Scargle periodogram of simulated light curve (bottom right). Simulated flux in watts/m^2.

This analysis validates the use of light curves as a way to assess the telemetry sensor readings. Nevertheless, the inverse problem, the extraction of body rates from the experimental light curves, doesn't have a unique solution and further study needs to be accomplished, as we find out that one particular value of body rate obtained from the simulated light curve correspond to different initial attitude and axes rotation rates.

We plan to address this problem with different techniques, among them, the observation of the spacecraft simultaneously from two different telescopes sited at two different geographical locations, which will reduce the number of possible initial cases, or the detailed study of the BRDF model to match the magnitudes of both the simulated flux and the experimental one. However, the estimation of orientation requires the shape information of the object. In addition, the relative difference in the reflectivity of the facet plays an important role for the estimation of the attitude orientation.

6 CONCLUSIONS AND FUTURE WORK

In this work a database of photometric light curves has been collected for the BRMM 3U CubeSat with corresponding attitude and position data available from the telemetry. Its preliminary analysis shows clear differences between the high and low body rate conditions. We can detect the deployment status of spacecraft structures, provided we have enough observations which cover all possible attitudes in the spacecraft. We have analysed the power spectra of both experimental and simulated light curves for passes of 5th and 6th of June 2018, using the Lomb-Scargle periodogram, which predicted the body rate to within the uncertainty of the telemetry data. These results indicate that experimental and simulated light curves can be used to assess the telemetry of the spacecraft, though the inverse problem, infer the attitude and body rates from the light curves will require further study. We plan to address this problem with techniques such as simultaneous observations from different telescopes, or the detailed study of the peaks magnitudes comparison of experimental and simulated light curves.

Future work will focus on the next actions:

- Quantification of the uncertainties in the spacecraft attitude determination.
- Influence of BRDF model, coefficients and material properties.
- Detailed comparison of light curves from pre and post solar panel/HF antenna deployment.
- Improvements in body rate and attitude estimation from fusing simulation data with multiples observations.

ACKNOWLEDGEMENTS

The authors would like to sincerely thank the entire BRMM operations team, comprising researchers and engineers from UNSW Canberra and DSTG Edinburgh, whose help, advice, and support was invaluable in planning the conduct of the experiments, with particular thanks to the DST operators for operating the spacecraft and downlinking the data during time sensitive periods. We would also like to extend our gratitude to Francis Chun and Kimberlee Gresham from USAFA for the donation of equipment, and the reliable support and coordination when using different nodes of the FTN network.

REFERENCES

1. https://www.nanosats.eu
2. Bianco G., Chersich M., Devoti R., Luceri V. and Selden M. Measurement of LAGEOS-2 Rotation by Satellite Laser Ranging Observations. *Geophysical Research Letters*, Vol. 28, No. 10, pages 2113-2116, 2001.
3. Lips T. et al, Debris Attitude Motion Measurements and modelling – Observation vs. Simulation. *Proceedings of AMOS Conference*, Maui, Hawaii, USA, September 19-22, 2017.
4. Pittet J-N. et al, Space Debris Attitude Determination of Faint LEO Objects using photometry: SwissCube CubeSat Study Case, *Proceedings of the 7th European Conference on Space Debris*, Darmstadt, Germany, Vol. 7, Issue 1, 2017
5. Gasdia F., Barjatya A. and Bilardi S., Time-resolved CubeSat Photometry with a Low Cost Electro-Optics System. *Proceedings of AMOS Conference*, Hawaii, US, 2016.
6. Ashikhmin, M., and Premože, S., "Distribution-based BRDFs," University of Utah Technical Report, 2007.
7. Griffin D., Lingard D., Boyce R., Young M., Brown M., Lambert A., DST Group and USNW Canberra Buccaneer Program. *Proceedings of the 68th IAC*, Adelaide, Australia, 25-29 Sept. 2017, paper: IAC-17-B4.2.6

8. https://directory.eoportal.org/web/eoportal/satellite-missions/content/-/article/buccane-1
9. Chun F. et al, A New Global Array of Optical Telescopes: The Falcon Telescope Network. *Publications of the Astronomical Society of the Pacific*, 130:095003 (20pp), 2018 September.
10. http://docs.astropy.org/en/stable/stats/lombscargle.html
11. Abay R., Gehly S., Brown M., Boyce R., High Area-To-Mass Ratio Object Characterization Using Machine Learning. 42nd COSPAR Scientific Assembly, Pasadena, California, 14-22 July 2018.